

GZ

• **CFD Modelling of Fluid and Heat Flow in Byron Common Header**

Technical Report

Prepared by Drs. S.V. Zhubrin and V. Agranat

from

Applied Computational Fluid Dynamics Analysis (ACFDA)

Thornhill, Ontario

for

AMAG Inc.

• March 2004

F-6

Introduction

This brief report summarises the results obtained from flow modelling of Byron Common Header Feedwater, using CFD.

The specification, provided by the client, is included as Appendix A.1.

Two cases were considered, with two different Inlet conditions and flow-rates.

The post-processing includes the calculation of Cf distribution (see Appendix A.1).

CFD Modelling

The supplied CAD drawing was used to generate an unstructured grid. The 3-D CAD model is shown in Fig. 1. Only half of the pipe was considered due to symmetry. The generated tetrahedral grid consists of:

| | |
|-------------------|---------|
| No. of Vertices : | 52,182 |
| No. of Faces: | 456,720 |
| No. of Cells: | 212,800 |

Figures 2-4 shows the grid at different locations of the pipe.

Figure 5 shows the axis system used, and the pipe orientation.

The problem was set-up for single-phase water with standard properties. The flow was considered to be turbulent, and the standard k- ϵ model was used for the calculations. The pipe walls were considered adiabatic, and the standard wall functions were applied.

The following variables were solved for :

KE, EP, X-Velocity, m/s, Y-Velocity, m/s, Z-Velocity, m/s, Pressure, N/m², Temperature, K, and PHI (concentration).

Convergence history of the calculation is depicted in Figure 6, showing the residuals of each variable solved for and, the values of X and Y-velocity components at one monitoring location.



Figure 1: CAD Geometry

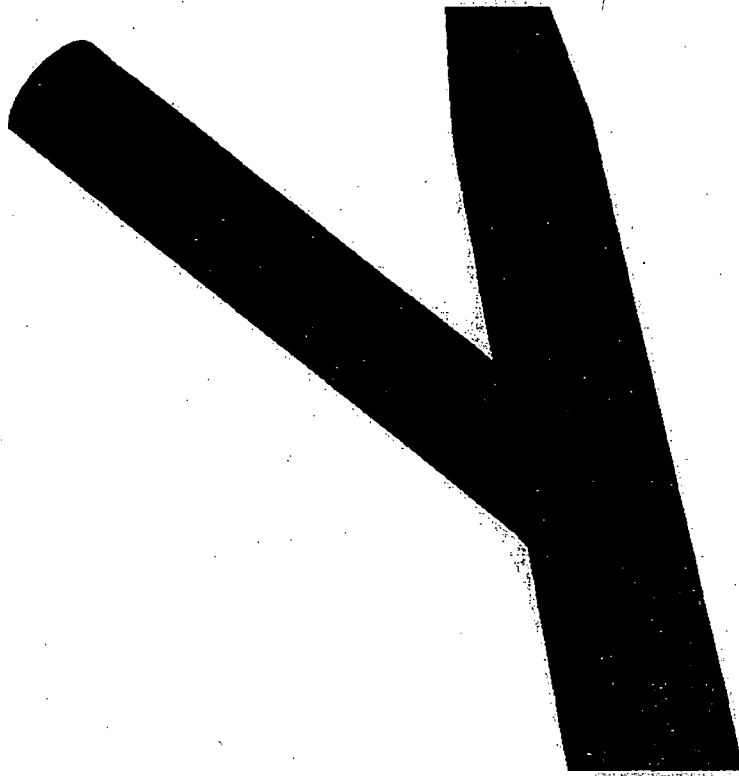


Figure 2: Fragment of computational mesh near Inlet-2

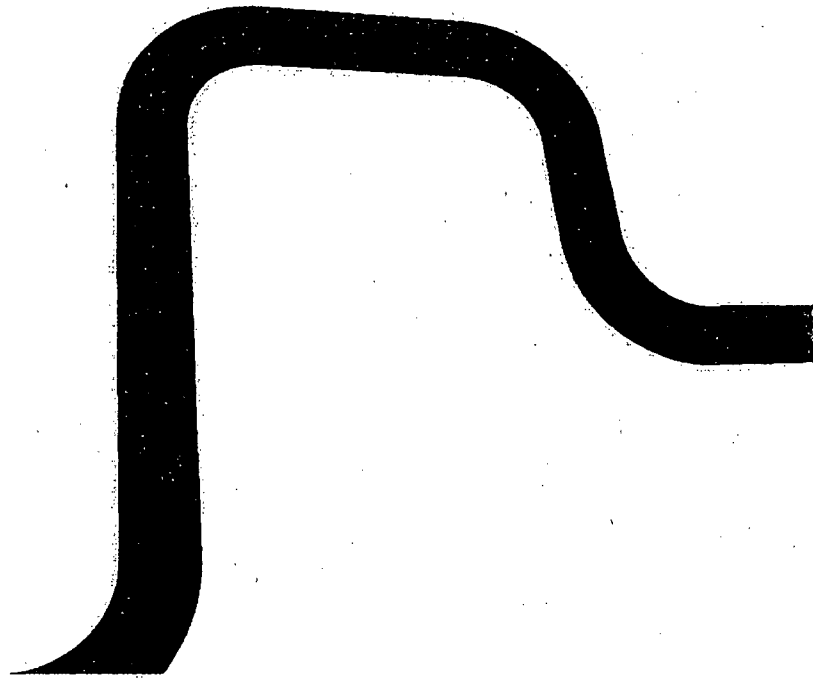


Figure 3: Fragment of computational mesh near elbows 3 and 4

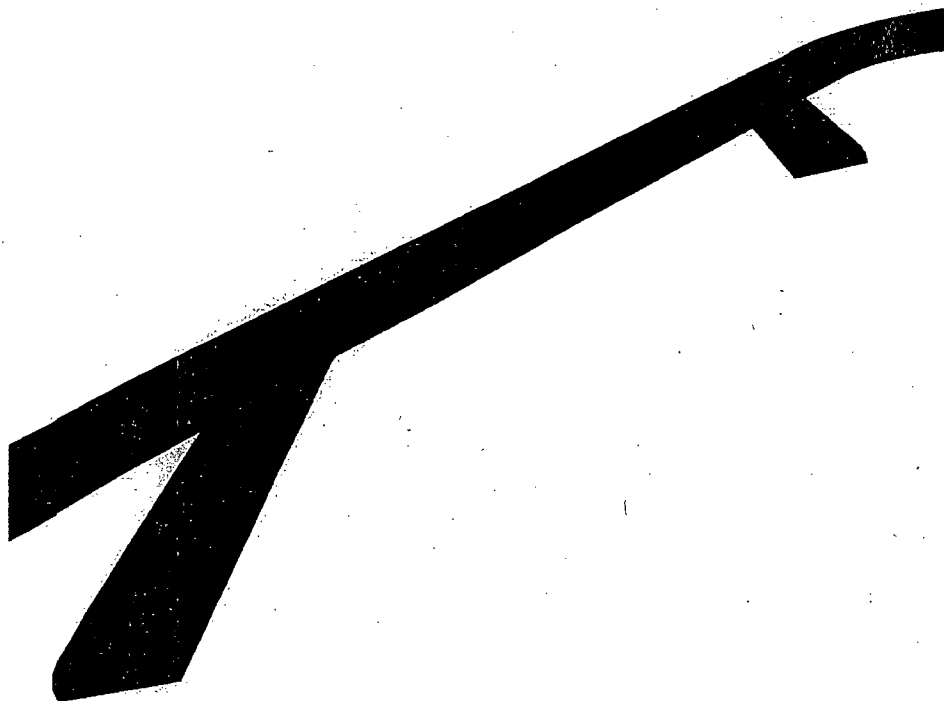


Figure 4: Fragment of computational mesh showing inlets 1 and 2

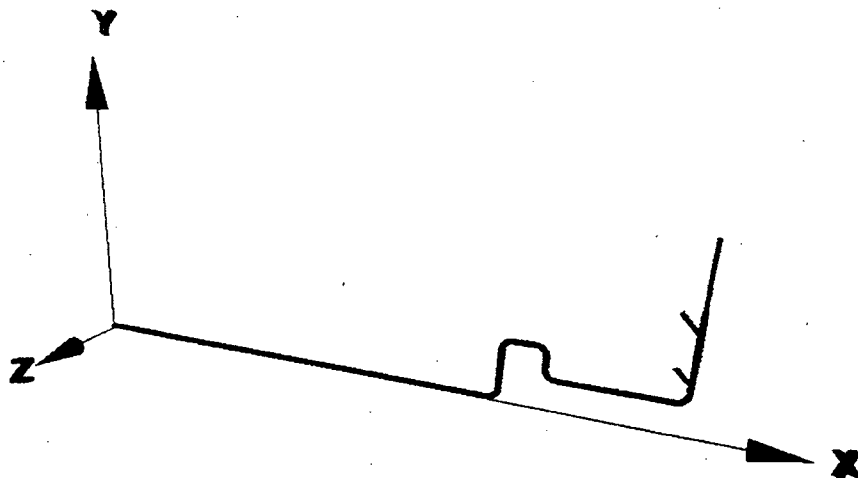


Figure 5: Coordinate system definition

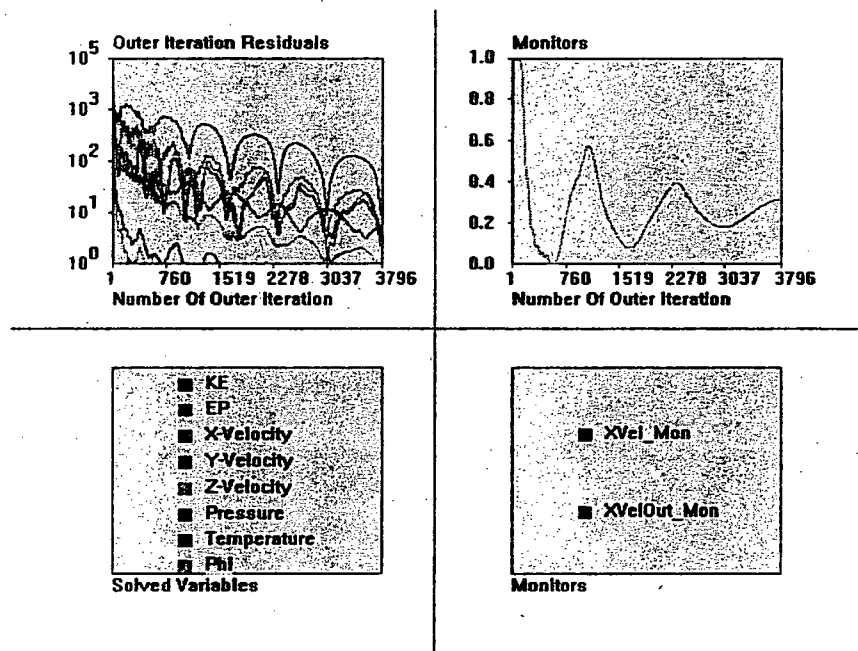


Figure 6: Convergence history and monitor graphs for Case-2

Results and Discussion

The results obtained from the two test-cases are presented in this section. The boundary conditions for both cases are presented in Appendix A.1.

Case-1:

Figure 7, shows the cross-section positions along the pipe, where the various solved variables have been plotted. Table-1, shows the C_f values at different sections.

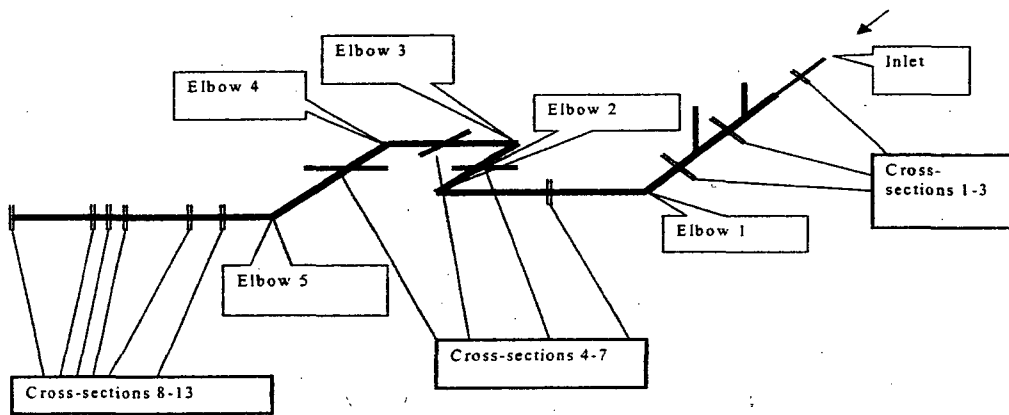


Figure 7: Positions of the Cross-sections, Inlets and Elbows

| Table-1: Case-1 | | | | | |
|------------------------|----------|----------|-----------|-----------|-----------|
| Section | 4 | 6 | 10 | 11 | 13 |
| C_{fy} | 1.02 | 0.995 | 1.0079 | 1.0097 | 1.0039 |
| C_{fz} | 0.99 | 0.993 | 1.003 | 1.0028 | 1.0022 |

Figure 8 shows results in Section-4 of the pipe. The pictures show the Cross-section of grid, the axial velocity distribution (m/s) and the projected velocity vector field on the cutting plane. The maximum velocity vector is 0.02 m/s. Figure 9 shows the concentration distribution at Section-4.

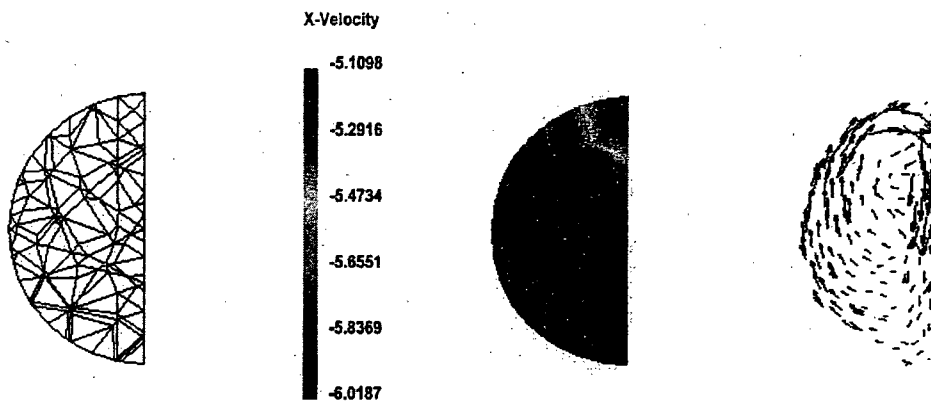


Figure 8: Velocity distribution for Case-1 at Section-4

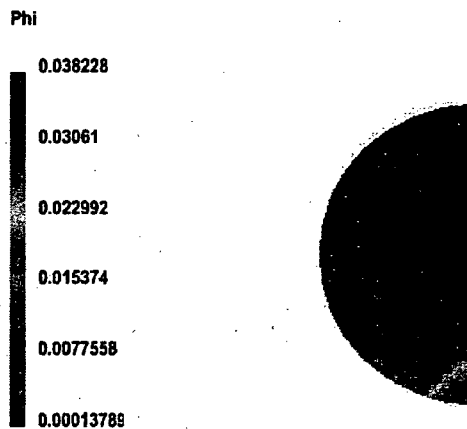


Figure 9: Concentration distribution for Case-1 at Section-4

Figure 10 shows results in Section-6 of the pipe. The pictures show the Cross-section of grid, the axial velocity distribution (m/s) and the projected velocity vector field on the cutting plane. The maximum velocity vector is 0.05 m/s. Figure 11 shows the concentration distribution at Section-6.

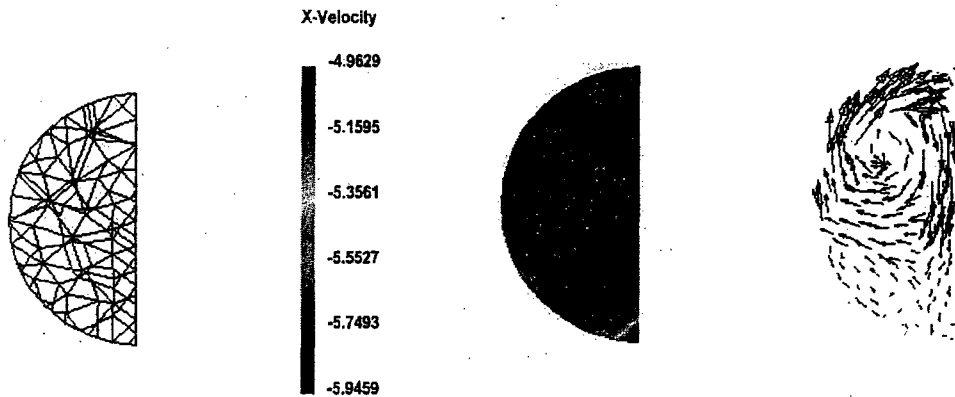


Figure 10: Velocity distribution for Case-1 at Section-6

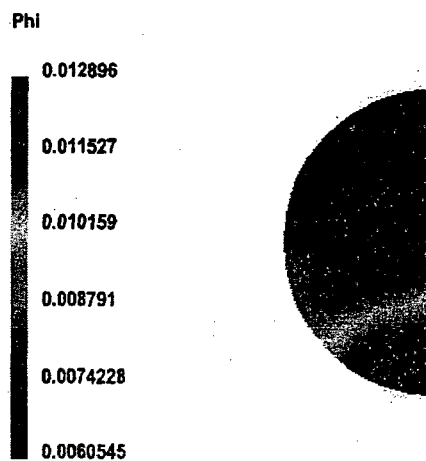


Figure 11: Concentration distribution for Case-1 at Section-6

Figure 12 shows results in Section-10 of the pipe. The pictures show the Cross-section of grid, the axial velocity distribution (m/s) and the projected velocity vector field on the cutting plane. The maximum velocity vector is 0.003 m/s. Figure 13 shows the concentration distribution at Section-10.

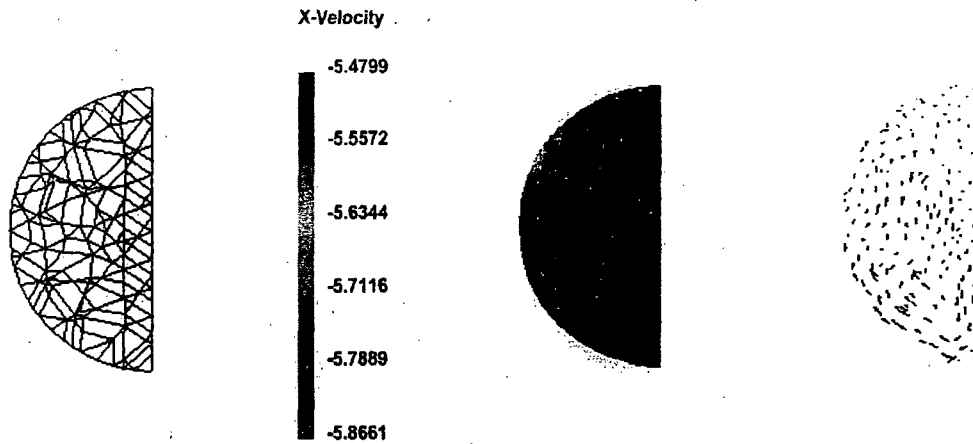


Figure 12: Velocity distribution for Case-1 at Section-10

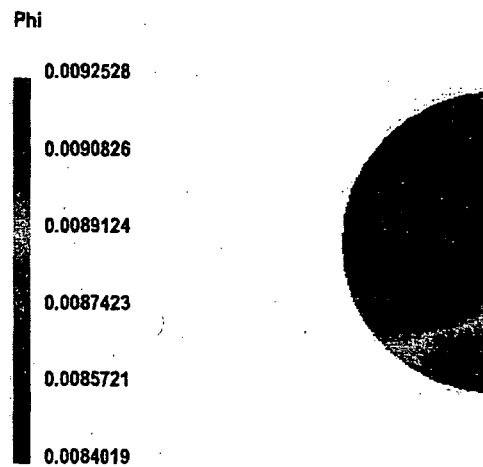


Figure 13: Concentration distribution for Case-1 at Section-10

Figure 14 shows results in Section-11 of the pipe. The pictures show the Cross-section of grid, the axial velocity distribution (m/s) and the projected velocity vector field on the cutting plane. The maximum velocity vector is 0.003 m/s. Figure 15 shows the concentration distribution at Section-11.

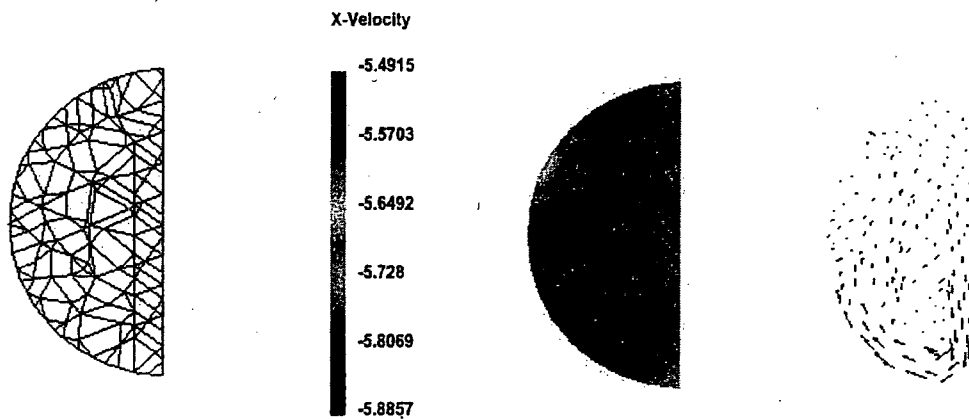


Figure 14: Velocity distribution for Case-1 at Section-11

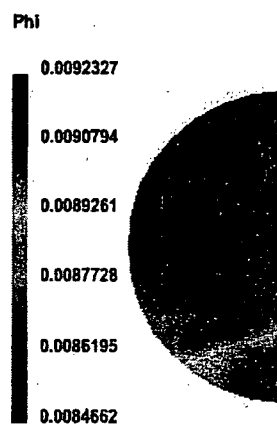


Figure 15: Concentration distribution for Case-1 at Section-11

Figure 16 shows results in Section-13 of the pipe. The pictures show the Cross-section of grid, the axial velocity distribution (m/s) and the projected velocity vector field on the cutting plane. The maximum velocity vector is 0.003 m/s. Figure 17 shows the concentration distribution at Section-13.

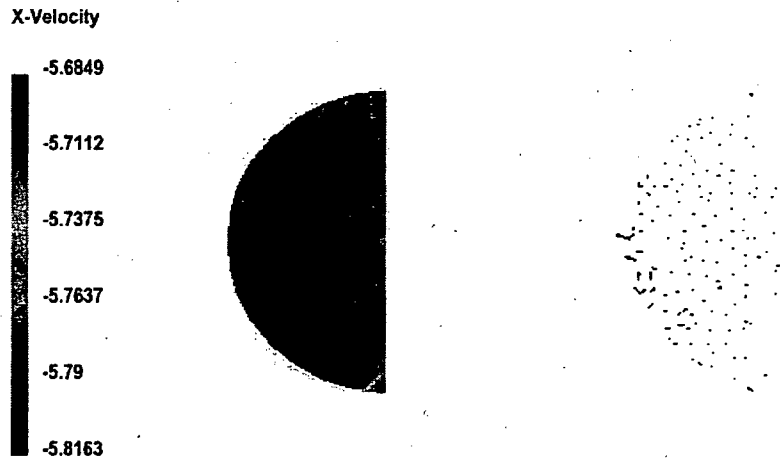


Figure 16: Velocity distribution for Case-1 at Section-13

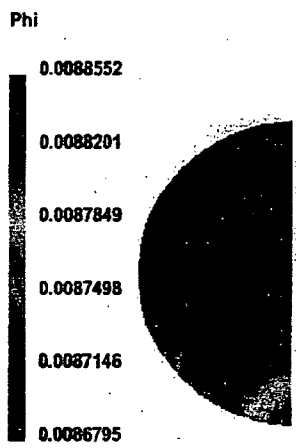


Figure-17: Concentration distribution for Case-1 at Section-13

Case-2:

Figure 7, shows the cross-section positions along the pipe, where the various solved variables have been plotted. For this case, temperature was calculated and results are presented. Table-1, shows the C_f values at different sections.

| Table-2: Case-2 | | | | | |
|-----------------|--------|--------|--------|--------|-------|
| Section | 4 | 6 | 10 | 11 | 13 |
| C_{fy} | 1.0064 | 0.995 | 0.99 | 0.99 | 0.997 |
| C_{fz} | 0.996 | 0.9947 | 0.9988 | 0.9996 | 0.998 |

Figure 18 shows results in Section-4 of the pipe. The pictures show the Cross-section of grid, the axial velocity distribution (m/s) and the projected velocity vector field on the cutting plane. The maximum velocity vector is 0.052 m/s. Figure 19 shows the concentration distribution and temperature distribution at Section-4.

X-Velocity

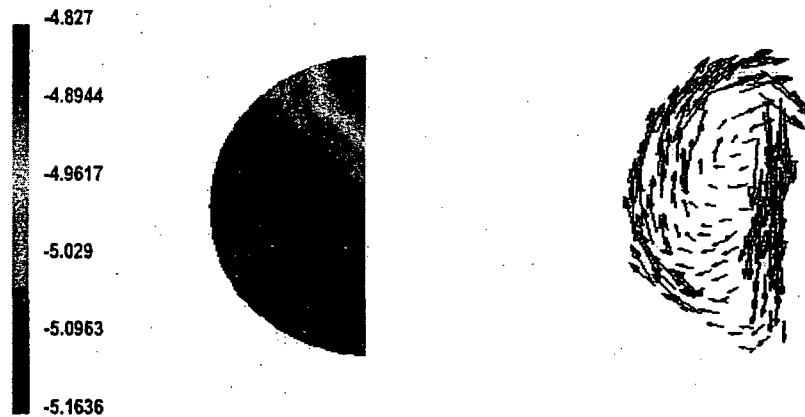


Figure 18: Velocity distribution for Case-2 at Section-4

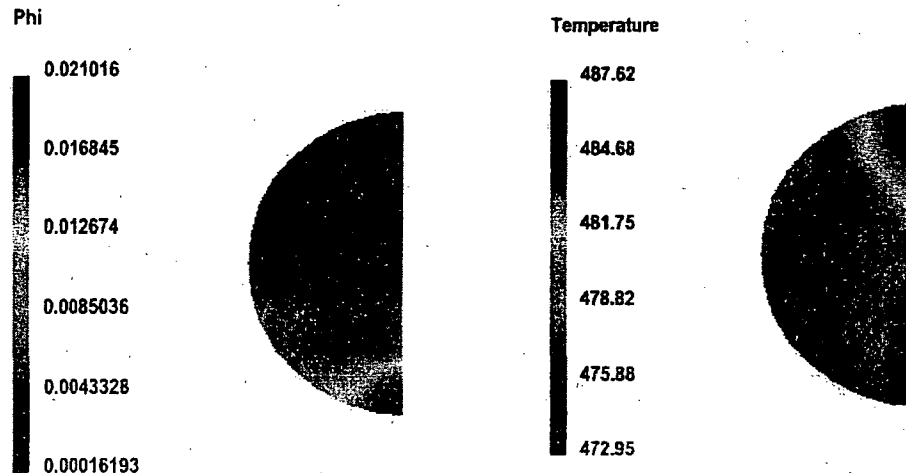


Figure 19: Concentration and temperature distribution for Case-2 at Section-4

Figure 20 shows results in Section-6 of the pipe. The pictures show the Cross-section of grid, the axial velocity distribution (m/s) and the projected velocity vector field on the cutting plane. The maximum velocity vector is 0.04 m/s. Figure 21 shows the concentration distribution and temperature distribution at Section-6.

X-Velocity

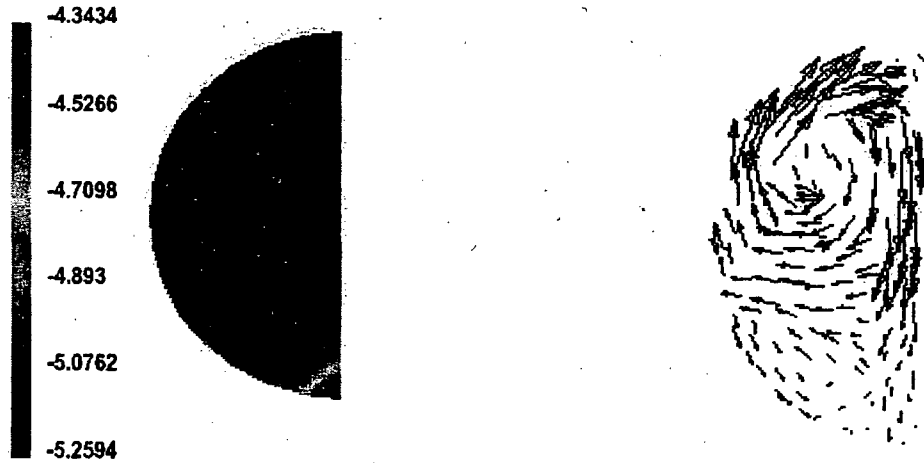


Figure 20: Velocity distribution for Case-2 at Section-6

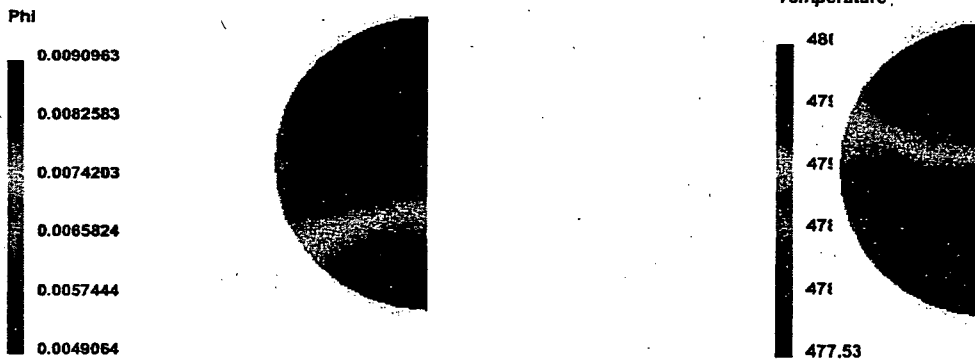


Figure 21: Concentration and temperature distribution for Case-2 at Section-6

Figure 22 shows results in Section-10 of the pipe. The pictures show the Cross-section of grid, the axial velocity distribution (m/s) and the projected velocity vector field on the cutting plane. The maximum velocity vector is 0.002 m/s. Figure 23 shows the concentration distribution and temperature distribution at Section-10.

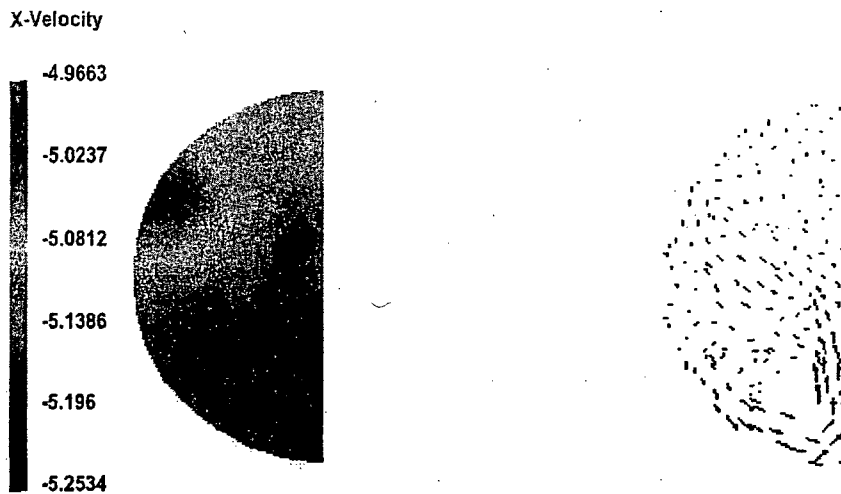


Figure 22: Velocity distribution for Case-2 at Section-10

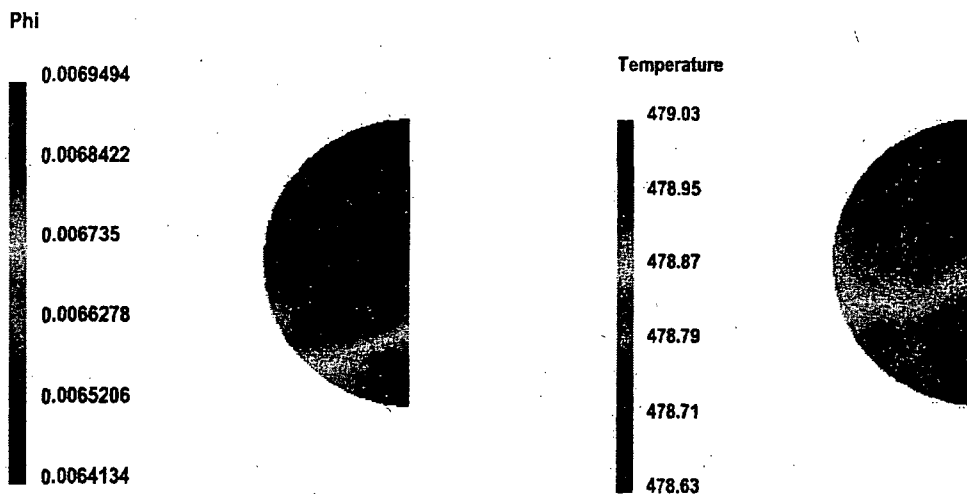


Figure 23: Concentration and temperature distribution for Case-2 at Section-10

Figure 24 shows results in Section-11 of the pipe. The pictures show the Cross-section of grid, the axial velocity distribution (m/s) and the projected velocity vector field on the cutting plane. The maximum velocity vector is 0.002 m/s. Figure 25 shows the concentration distribution and temperature distribution at Section-11.

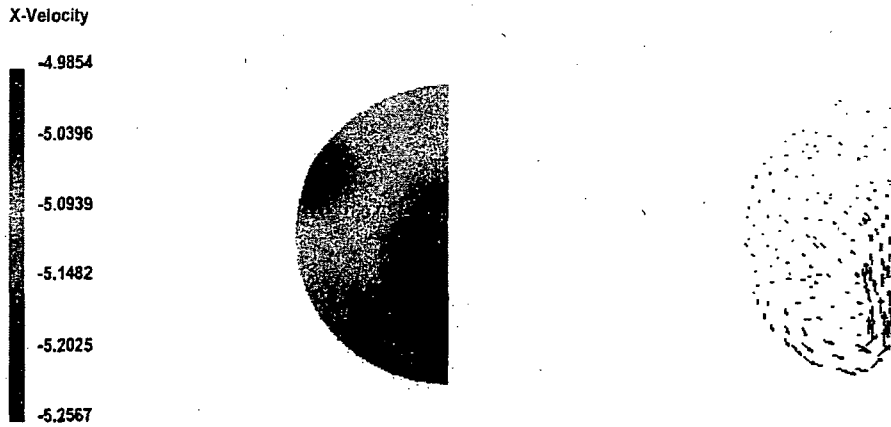


Figure 24: Velocity distribution for Case-2 at Section-11

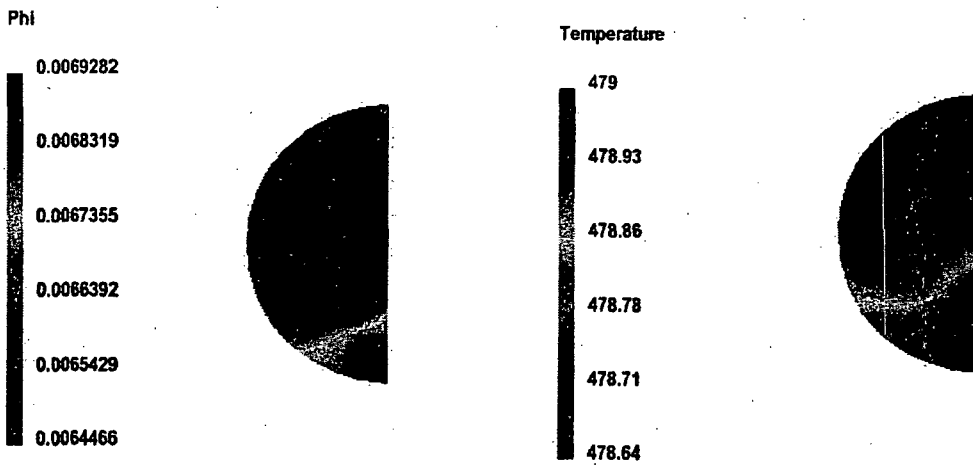


Figure 25: Concentration and temperature distribution for Case-2 at Section-11

Figure 26 shows results in Section-13 of the pipe. The pictures show the Cross-section of grid, the axial velocity distribution (m/s) and the projected velocity vector field on the cutting plane. The maximum velocity vector is 0.002 m/s. Figure 27 shows the concentration distribution and temperature distribution at Section-13.

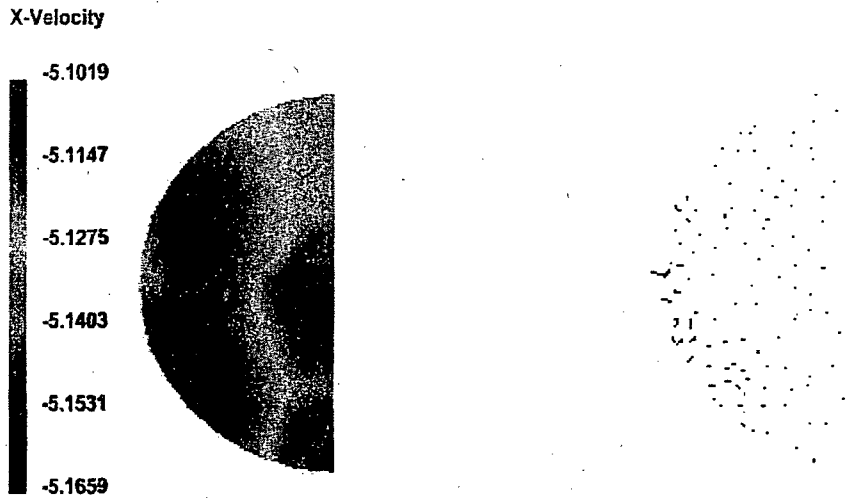


Figure 26: Velocity distribution for Case-2 at Section-13

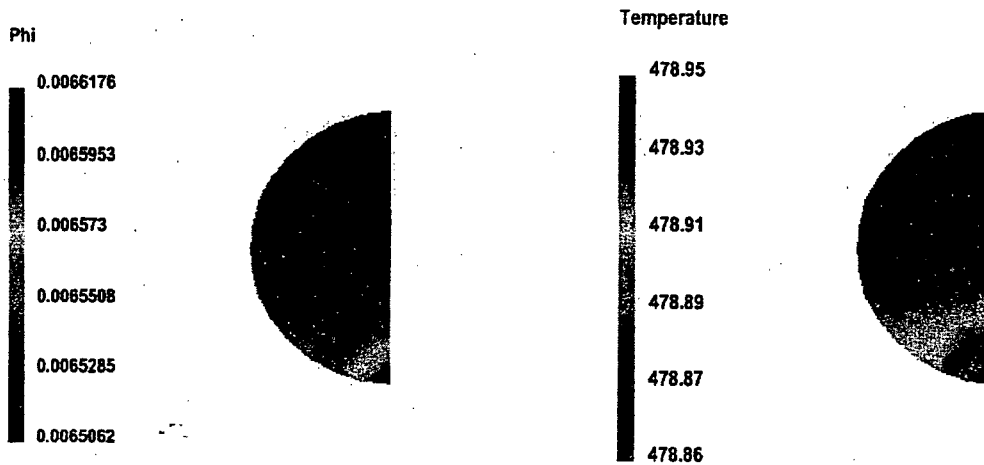


Figure 27: Concentration and temperature distribution for Case-2 at Section-13

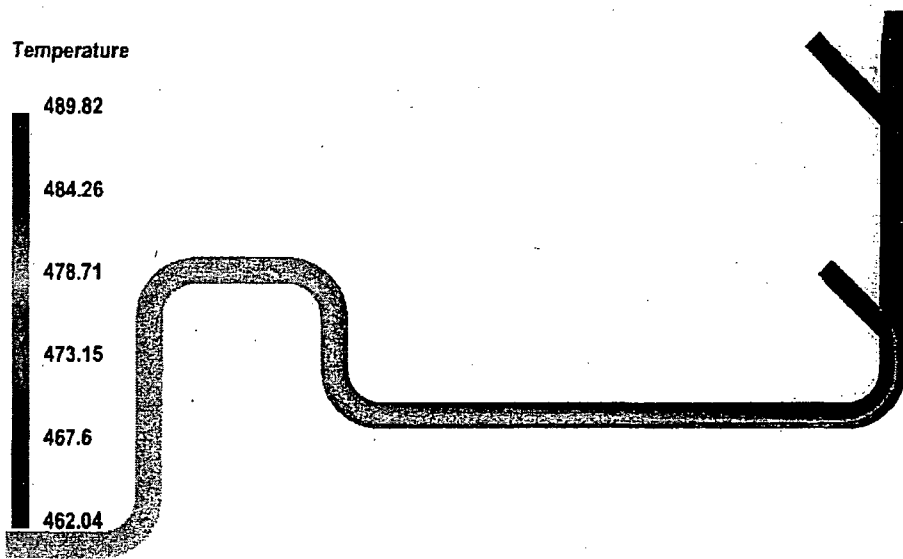


Figure 28: Temperature distribution on the symmetry plane for Case-2

Appendix A.1: Specification provided by client

CFD Specification for Byron Common Header Feedwater Flow Modeling

1. Position of the cross-sections with output of the results of calculations

The number, starting from the pipe inlet, identifies each 90-degree elbow and flow inlets (see Figure 7).

The distance along pipe axis defines position of a cross-section.

For cross-sections upstream of the Elbow 1, the distance is counted from the inlet of the 17" pipe

For cross-sections downstream of the Elbow 1, the distance is counted from the nearest upstream elbow along centerline of the pipe.

Position of an elbow is defined as a position of the intersection point of the centerlines of the pipes.

Positions of the cross-sections are defined in Table 1 and are illustrated in Figure 7.

Table 1. Positions of the cross-sections with output of the CFD results

| Cross-section ID | Distance from inlet (inches) | Comments |
|-------------------------|-------------------------------------|--|
| Cross-section 4 | 270 (counted from Elbow 1) | Downstream of the Elbow 1 Approximately in the middle, between Elbow 1 and Elbow 2 |
| Cross-section 6 | 88 (counted from Elbow 3) | Downstream of the Elbow 3 Approximately in the middle, between Elbow 3 and Elbow 4 |
| Cross-section 10 | 602.127 (counted from Elbow 5) | 23.07 pipe diameters from Elbow 5. Corresponds to Byron U2 installation |
| Cross-section 11 | 710.964 (counted from Elbow 5) | 27.24 pipe diameters from Elbow 5. Corresponds to Byron U1 installation |
| Cross-section 13 | 1044 (counted from Elbow 5) | 40 pipe diameters from Elbow 5 |

2. Input Parameters and Boundary Conditions

CFD modeling has to be conducted for single-phase water with standard properties.
Some cases include inlet streams with different temperature.

Case # 1

Total flow rate - 15700 klbm/h

Flow Temperature: 422F

Flow Pressure: 1224.5 psi

Flow is evenly distributed between Inlet 2 and Inlet 3 with the same temperature and pressure. No flow in Inlet 1.

The passive tracer injection point is located on the wall of the main pipe, opposite to the Inlet 3. The concentration of the passive tracer is equal to 1. The area of injection equals to the area of one grid cell of the CFD model.

For this case, the Cross-section 1 should not be considered.

Case # 2

Total flow rate is 14130 klbm/h
 Inlet 1 conditions: Flow rate 5652 klbm/h
 Flow temperature 372F
 Flow Pressure 1224.5 psi
 Inlet 2 conditions: No Flow
 Inlet 3 conditions: Flow rate - 8478
 Flow Temperature 422F
 Flow Pressure 1224.5 psi

The passive tracer injection point is located on the wall of the main pipe, opposite to the Inlet 3 (the same as in Case # 1). The concentration of the passive tracer is equal to 1. The area of injection equals to the area of one grid cell of the model.

3. Output Parameters

In each specified above cross-section, the results of the modeling have to be presented as follows:

Graphical Presentation:

- Axial, angular and radial velocity distributions along pipe diameter in horizontal and vertical directions.
- Axial velocity distribution, passive tracer concentration distribution and temperature distribution (for Case # 2) in the form of constant value lines in two-dimensional space.
- Vector diagram of the projection of the velocity vector on the cross-section.
- Cf distribution, as a function of angle in each specified cross-section, and Cf distributions along pipe axis, where Cf is calculated in vertical and horizontal orientations.

Cf is defined as follows:

U - axial velocity component

U_a - cross-section average axial velocity (Constant)

μ_t - effective turbulent viscosity

D - pipe diameter

r - coordinate, which is counted along pipe diameter, starting from pipe wall.

θ - angular coordinate

x - coordinate along pipe axis

$$C_f(x, \theta) = \frac{1}{U_a} \frac{\int_0^D U(x, r, \theta) \cdot \mu_t(r, \theta) dr}{\int_0^D \mu_t(x, r, \theta) dr}$$

